Magnetic Diffusion Modeling In Nonlinear Micro-Media: A Modified Finite-Difference Time-Domain Approach

H. Köşer*, F. Cros**, M. G. Allen** and J. H. Lang*

* Massachusetts Institute of Technology,
36-873, 50 Vassar St., Cambridge, MA 02139, USA, hurkoser@alum.mit.edu
** Microelectronics Research Center, Georgia Institute of Technology, Atlanta, GA 30332, USA

ABSTRACT

As flux densities and frequencies are raised to increase the performance of magnetic actuators, machines, and inductors in the micro-scale, eddy currents and magnetic saturation start to limit the performance of these devices. In this paper, we present a powerful numerical method based on a modified finite-difference time-domain simulation of Maxwell's equations. This method successfully models both eddy currents and material saturation within a magnetic MEMS device. Experimental verification of the method is also presented.

Keywords: Power MEMS, induction machine, magnetic diffusion, FDTD.

1 INTRODUCTION

Conventional magnetic machines are finely laminated to reduce eddy current effects. At the micro scale, however, laminations increase fabrication complexity and decrease magnetic material density. To compromise, it is necessary to study device performance in the presence of eddy currents and saturation. Such studies of AC magnetic devices cannot always be reliably conducted with conventional commercial finite-element software, as they typically simulate only the fundamental harmonic of exciting currents and the resulting magneto-quasistatic response, which may lead to gross inaccuracies. Improved algorithms, such as the Shooting Method [1] and the Generalized Minimum Residuals approach based on matrix-free Krylov-subspace methods [2] are accurate yet computationally expensive – taking on the order of days to complete. In order to be practical during device design and analysis, a nonlinear simulation tool for magnetic diffusion needs to be both accurate and very fast – less than an hour per simulation.

We present a novel numerical method to solve for nonlinear magnetic diffusion based on an explicit finite-difference time-domain (FDTD) integration of Maxwell's equations [3]. The approach is combined with an artificial reduction in the speed of light [4], which reduces stiffness in the partial differential equations (PDEs) and dramatically speeds up the process. Experimental verification of the modified FDTD method is provided through torque measurements on a magnetic induction micro motor [5], [6] (Figure 1).

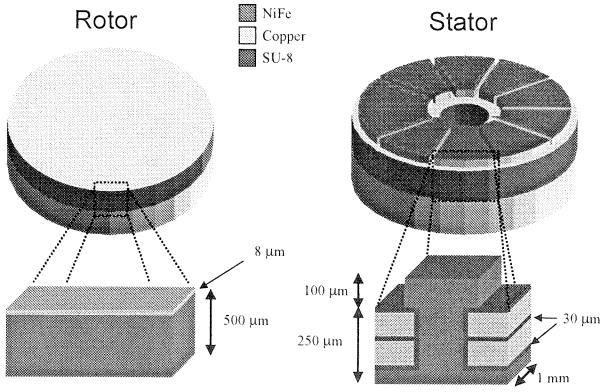

Figure 1: Schematic of the magnetic induction micro machine, and some relevant dimensions. The rotor is supported above the stator by six tethers (not shown here) whose deflections are used to determine motoring torque.

2 DISCRETIZATION SETUP

We exploit the axial symmetry of the micro motor by solving for electromagnetic fields in radial cross-sections as mapped onto a two-dimensional Cartesian plane. The stator consists of two windings excited in quadrature, which means the traveling excitation goes through one wavelength over four wire slots. Hence, it suffices to simulate over the extent of just two wire slots, as the rest of the motor can be simulated with odd symmetric boundary conditions on either side. Figure 2 illustrates the computation space and the discretization scheme. Consider the full set of Maxwell's Equations

$$\epsilon\frac{\partial \mathbf{E}}{\partial t} + \sigma\mathbf{E} + \mathbf{J}_{\text{ext}} = \nabla \times \mathbf{H} \quad \text{(Ampere)} \quad (1)$$

$$\frac{\partial \mathbf{B}}{\partial t} = -\nabla \times \mathbf{E} \quad \text{(Faraday)} \quad (2)$$

$$\mathbf{H} = \frac{1}{\mu}\mathbf{B} \quad \text{(Material)} \quad (3)$$

with the convention that in those locations where a source sets the total current density, the $\sigma\mathbf{E}$ term is not present. It is assumed that the $\mathbf{E}$ and $\mathbf{B}$ fields will be divergence-free by construction (see below). Due to the two dimensional nature of the problem, we need only

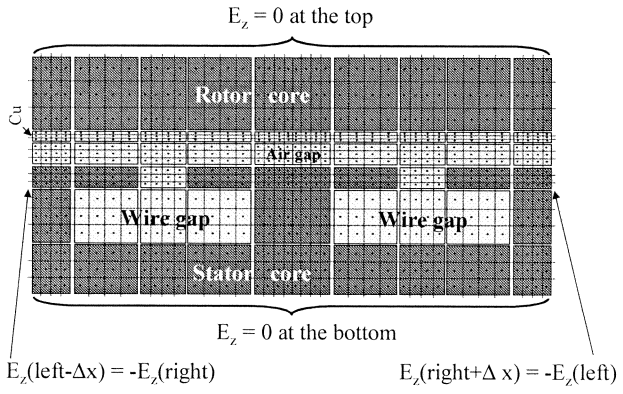

Figure 2: The smallest computation space needed for the FDTD scheme. For clarity, a diffuse mesh is shown.

to consider the magnetic field components along the x-y plane in Figure 2, and the electric field component perpendicular to that plane.

2.1 Electric field update

Let us integrate Equation 1 over the surface S_{ij} of a given unit cell on the x-y plane at location (x_i, y_j), and convert the RHS into a line integral along C_{ij} around the unit cell. This yields

$$\int_{S_{ij}} \left(\epsilon \frac{\partial \mathbf{E}}{\partial t} + \sigma \mathbf{E} + \mathbf{J}_{\text{ext}} \right) \cdot d\mathbf{S} = \int_{C_{ij}} \mathbf{H} \cdot d\mathbf{l} \qquad (4)$$

The standard FDTD algorithm [3] calls for a discretization scheme in which magnetic and electric field points are separated both in space and time by half a discretization (Figure 3). We shall evaluate electric field values

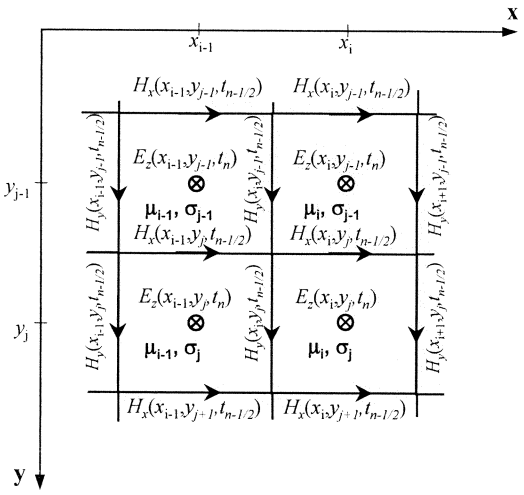

Figure 3: The general meshing scheme used in an FDTD algorithm.

at integer multiples of the time step, and find magnetic field values half a time step later, in a leap-frogging manner. This method ensures that first order finite differences for derivates are second order accurate. Moreover, the finite difference grid, with each electric field point encircled by magnetic field lines, is divergence-free (both in $\mathbf{E}$ and $\mathbf{B}$) by construction [7].

Let us continue by evaluating Equation 4 at time step $n-\frac{1}{2}$. Here, we shall represent $\epsilon \frac{\partial \mathbf{E}}{\partial t}\Big|^{n-\frac{1}{2}}$ as $\epsilon \left(\frac{\mathbf{E}^n - \mathbf{E}^{n-1}}{\Delta t} \right)$, and use a semi-implicit approximation to write $\sigma \mathbf{E}|^{n-\frac{1}{2}}$ and $\mathbf{J}_{\text{ext}}|^{n-\frac{1}{2}}$ as $\sigma \left(\frac{\mathbf{E}^n + \mathbf{E}^{n-1}}{2} \right)$ and $\left(\frac{\mathbf{J}^n_{\text{ext}} + \mathbf{J}^{n-1}_{\text{ext}}}{2} \right)$, respectively. Collecting terms, we get

$$\begin{aligned} E^n_{z_{ij}} &= \left[1 - \beta_{ij}\,(2/\sigma_{ij})\right] E^{n-1}_{z_{ij}} \\ &\quad + \beta_{ij}\,(\Delta x_{ij}) \left(H^{n-\frac{1}{2}}_{y_{i+1,j}} - H^{n-\frac{1}{2}}_{y_{ij}} \right) \\ &\quad - \beta_{ij}\,(\Delta y_{ij}) \left(H^{n-\frac{1}{2}}_{x_{i,j+1}} - H^{n-\frac{1}{2}}_{x_{ij}} \right) \\ &\quad - \beta_{ij}\,(2) \left(J^n_{\text{ext}_{ij}} + J^{n-1}_{\text{ext}_{ij}} \right) \end{aligned} \qquad (5)$$

where the function

$$\beta_{ij}\,(a) = \left(\frac{\Delta t}{a \epsilon_{ij}} \right) / \left(1 + \frac{\Delta t \sigma_{ij}}{2 \epsilon_{ij}} \right) \qquad (6)$$

has been defined for notational convenience.

2.2 Magnetic field update

We need another equation to find the magnetic field values at each spatial location; for that, we shall employ Faraday's law and follow the same approach as above. In order to convert the curl of the electric field into a line integral, the contours must be around a surface S'_{ij} pointing along the $\hat{\mathbf{y}}$ direction (Figure 4). We begin by

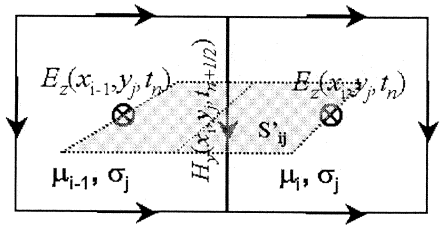

Figure 4: Surface for magnetic field update.

integrating both sides of Equation 2 over the surface S'_{ij} of Figure 4 at time step n to obtain

$$\int_{S'_{ij}} \frac{\partial \mathbf{B}}{\partial t}\Big|^n \cdot d\mathbf{S}' = -\int_{C'_{ij}} \mathbf{E}|^n \cdot d\mathbf{l}' \qquad (7)$$

One must pay special care in evaluating the LHS of Equation 7, since both the material properties and the flux density field values are not uniform over the surface

of integration. Evaluation then yields

$$\frac{B_{y_{i-1,j}}^{n+1/2} - B_{y_{i-1,j}}^{n-1/2}}{\Delta t}\Delta x_{i-1,j} + \frac{B_{y_{ij}}^{n+1/2} - B_{y_{ij}}^{n-1/2}}{\Delta t}\Delta x_{ij} = \left(E_{z_{ij}}^{n} - E_{z_{i-1,j}}^{n}\right) \quad (8)$$

We can solve for $B_{y_{ij}}^{n+1/2}$ by using the continuity of H_y across tangential material interfaces, which implies $\mu_{i-1,j}^{n+1/2} B_{y_{i-1,j}}^{n+1/2} = \mu_{ij}^{n+1/2} B_{y_{ij}}^{n+1/2}$. The problem is that we do not yet know what μ_{ij} is at time step $n+\frac{1}{2}$, as we would first need both $B_{x_{ij}}^{n+1/2}$ and $B_{y_{ij}}^{n+1/2}$ to find it. Short of solving a matrix inversion problem, this implicitness may be mitigated by using $\mu_{ij}^{n-1/2}$ as the initial guess for $\mu_{ij}^{n+1/2}$ and iterating Equation 8 between the flux density and the permeability until $\mu_{ij}^{n+1/2}$ eventually converges. Depending on the size of the time step, a few such iterations generally suffice. Nevertheless, the time step, Δt, is often so small that approximating $\mu_{ij}^{n+1/2} \approx \mu_{ij}^{n-1/2}$ here for the purposes of Equation 8 works quite well, yielding

$$B_{y_{ij}}^{n+1/2} = B_{y_{ij}}^{n-1/2} + \gamma_{ij}^{n-1/2}\left(\Delta x_{ij}\right)\left(E_{z_{ij}}^{n} - E_{z_{i-1,j}}^{n}\right) \quad (9)$$

where

$$\gamma_{ij}^{n-1/2}\left(\Delta x_{ij}\right) = \Delta t\left[\frac{\mu_{i-1,j}^{n-1/2}}{\mu_{ij}^{n-1/2}}\left(\frac{\Delta x_{i-1,j}}{2}\right) + \frac{\Delta x_{ij}}{2}\right]^{-1} \quad (10)$$

is defined for notational simplicity.

Magnetic flux density along the $\hat{\mathbf{x}}$ direction at unit cell (i,j) can be found in exactly the same manner as above. The update equation for B_x is

$$B_{x_{ij}}^{n+1/2} = B_{x_{ij}}^{n-1/2} - \gamma_{ij}^{n-1/2}\left(\Delta y_{ij}\right)\left(E_{z_{ij}}^{n} - E_{z_{i,j-1}}^{n}\right) \quad (11)$$

2.3 Magnetic permeability update

Now that the $\mathbf{B}$ field is known everywhere at time $t = \left(n+\frac{1}{2}\right)\Delta t$, the magnetic permeability of NiFe across the computational grid is updated using a look-up table based on the measured magnetization curve of the material. Given $|\mathbf{B}|$, $|\mathbf{H}|$ and hence $\mu\left(|\mathbf{B}|\right)$ are found by direct interpolation. Care is taken to ensure that the magnetic field and the magnetic flux density vectors are collinear.

3 IMPLEMENTATION ISSUES

The largest time step that we can choose is determined by the Courant stability condition [7], and depends on the particular numerical resolution of the excitation speed within the discretization scheme. In the simplest case of a one-dimensional uniform grid with linear materials,

$$\Delta t \leq \frac{\Delta x}{c} \quad (12)$$

is a necessary (but not sufficient) condition to guarantee stability. With nonlinear media in two dimensions, the bound is even tighter. What is more, the minimum Δx must be much shorter than the shortest wavelength or characteristic distance (such as skin depth) present in the problem. In the case of the micro motor geometry and its high operating frequencies, this constraint translates to a time step on the order of femtoseconds.

The tight constraint on stability arises from the inherent stiffness in the PDEs: electromagnetic waves travel essentially at the speed of light $(1/\sqrt{\mu_o \epsilon_o})$ in air, yet the magnetic diffusion waves travel much slower $(\sqrt{\omega/\mu_s \sigma_s})$ inside NiFe – up to three hundred thousand times slower than light. Here, we adopted an implementation in which the speed of light has been artificially reduced many orders of magnitude, in order to reduce the stiffness of the PDEs. Since the emphasis is on magnetic diffusion phenomena, the reduction of c involves increasing the electric permittivity of all materials in our computation space [4], without altering their magnetic permeabilities. Care is taken to make sure that c is still many times faster than both the input traveling wave and the magnetic diffusion waves within all materials. This approach has enabled a stable time step as large as 2 ns – more than a sixty thousand times improvement. With this method, a simulation takes less than half an hour to conclude on an average PC. To give a perspective, the same simulation would have taken about seven years without the modification.

4 RESULTS

Torque output from the micro motor is calculated by integrating the Maxwell Stress Tensor around the rotor section in the computation space of Figure 2 to find the shear force acting on the rotor. At a given radius, the computed shear force is multiplied by the number of poles to obtain the torque per unit depth at that radius:

$$\tau_{xy}^{n+1/2} = p\sum_{i,j=j_o} \mu_0 H_{x_{i,j_o}}^{n+1/2} H_{y_{i,j_o}}^{n+1/2} \Delta x_{i,j_o} \quad (13)$$

where p is the number of stator poles (six in our case), and j_o is the ordinate index of the cell bordering air just on the rotor conductor. Several simulations at different radii are performed, and the total torque is approximated through a trapezoidal sum, which yields the instantaneous torque acting on the rotor. The steady-state value is extracted from the mean torque once the simulation settles, and the values are compared to experimentally measured torque values from the tethered magnetic induction micro motor.

Recreating the exact experimental conditions in numerical simulations is not possible. For one thing, our model is only a two-dimensional approximation of the micro machine. Three-dimensional effects such as eddy currents turning corners at the inner and outer radii are not captured in our model. Another issue is that local nonuniformities in each material's set of properties – such small voids within the electroplated NiFe – are not considered in these simulations. Moreover, parameters such as dimensions and operating temperature vary across the micro motor, and using their average values is yet another approximation. Nevertheless, the results of the FDTD algorithm still agree very well with the measured data, as illustrated in Figure 5. Results from a commercial magnetics package which uses matrix methods based on single harmonic assumptions are provided in Figure 6 for comparison.

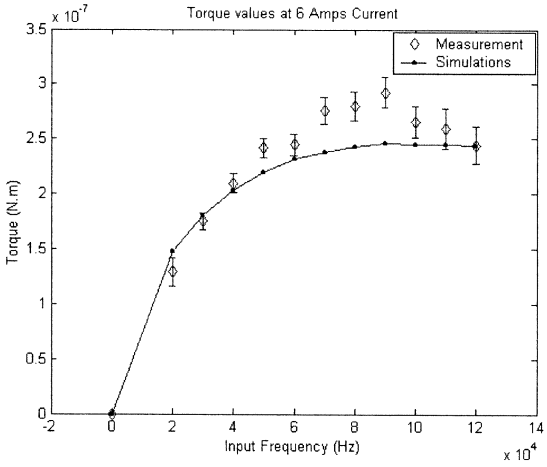

Figure 5: Experimental data (with 6A AC current input in each phase) from the tethered magnetic micro-motor, and the corresponding simulation results from the nonlinear FDTD model.

5 CONCLUSIONS

In this paper, we present a modeling methodology for studying magnetic diffusion in nonlinear media. The approach is based on a fully nonlinear, explicit finite-difference time-domain solution of Maxwell's equations. In order to speed up the computation, the speed of light is artificially reduced (through increasing the dielectric permittivity everywhere) to a point where stiffness inherent in the equations is mitigated. Using this method, we have computed time-evolution of magnetic fields and field densities within a magnetic induction micro motor, and compared resulting steady-state torque values to experimentally measured performance data. The results from this model match measurements very well, confirming the validity and the accuracy of the approach.

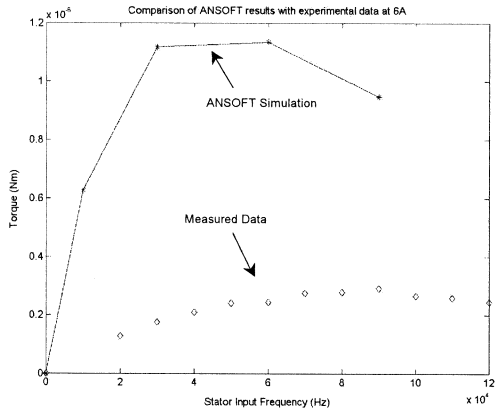

Figure 6: Commercially available magnetic simulation packages, such as ANSOFT, assume that only the fundamental excitation frequency contributes to magnetic diffusion in the presence of eddy currents and material nonlinearities. This assumption is not valid in cases where material nonlinearities are prominent.

It is worthwhile to point out that the solution methodology introduced here is applicable to nonlinear electroquasistatic effects in micro-media as well. The dual implementation in the electric domain involves a time-dependent electrical permittivity and a magnetic permeability that is scaled up to allow large time-steps.

6 ACKNOWLEDGMENTS

This work is supported by ARO grant DAAG55-98-1-0292, Dr. Thomas L. Doligalski, scientific officer.

REFERENCES

[1] Granas, A., Guenther, R. B., and Lee, J. W., SIAM Journal on Numerical Analysis, vol.16, no.5, pp.828-836, Oct. 1979.

[2] Li, S., and Hofmann, H., IEEE International Electric Machines and Drives Conf., Piscataway, NJ, x+1004, pp.275-279, 2001.

[3] Yee, K. S., IEEE Trans. Antennas and Propagation, vol. 14, pp. 302-307, 1966.

[4] Holland, R., IEEE Trans. On Electromagnetic Compatibility, vol. 36, no. 1, pp. 32-39, February 1994.

[5] Köşer, H. and Lang, J. H., Proceedings of International Conf. On Modeling and Simulation of Microsystems, pp. 286-289, Hilton Head Island, South Carolina, March 2001.

[6] Köşer, H. et al., Proceedings of the 11th International Conference on Solid-State Sensors and Actuators, Munich, Germany, June 2001.

[7] Taflove, A., "Computational Electrodynamics", Artech House, MA, 1995.